International Journal of Coal Geology 127 (2014) 88–99

Contents lists available at ScienceDirect

International Journal of Coal Geology

journal homepage: www.elsevier.com/locate/ijcoalgeo

Outlining of high quality coking coal by concentration–volume fractal model and turning bands simulation in East-Parvadeh coal deposit, Central Iran

Peyman Afzal [a,b,*], Seyed Hosein Alhoseini [b], Behzad Tokhmechi [c], Dariush Kaveh Ahangaran [a,b], Amir Bijan Yasrebi [a], Nasser Madani [d,e], Andrew Wetherelt [a]

[a] Camborne School of Mines, University of Exeter, Penryn, UK
[b] Department of Mining Engineering, Faculty of Engineering, South Tehran Branch, Islamic Azad University, Tehran, Iran
[c] School of Mining, Petroleum and Geophysics Engineering, Shahrood University, Shahrood, Iran
[d] Department of Mining Engineering, University of Chile, Santiago, Chile
[e] Advanced Mining Technology Center, University of Chile, Santiago, Chile

ARTICLE INFO

Article history:
Received 31 December 2013
Received in revised form 7 March 2014
Accepted 8 March 2014
Available online 25 March 2014

Keywords:
Concentration–volume (C–V) fractal model
Turning bands simulation
Logratio matrix
Sulfur
Ash
East-Parvadeh

ABSTRACT

This study aims at identifying the proper parts of C_1 and B_2 coking coal seams in the North block of East-Parvadeh coal deposit (Central Iran) using the concentration–volume (C–V) fractal modeling according to sulfur and ash values which were calculated by turning bands conditional simulation. The C–V log–log plots were generated based on results of 100 realizations derived via turning bands simulation which show seven different geochemical populations for both sulfur and ash data in B_2 seam which has a relatively good quality for coking coal with sulfur and ash values lower than 1.548% and 6.39% respectively. Additionally, C–V log–log plots indicate that there are seven and six for sulfur and ash geochemical populations in C_1 seam containing a proper coal quality with respect to sulfur and ash values less than 1.41% and 6.92% respectively. High quality populations are located in the northern and western parts of the studied area which correlated with USGS standard. The logratio matrix was used for the correlation between results obtained by the C–V fractal modeling and geological particulars consisting of pyritic veins and ash coals. Based on the logratio matrix for sulfur values higher than 3.55% and 3.39% for C_1 and B_2, respectively, low quality parts of the seams have good correlation with pyritic veins in the eastern and central parts of the area. Moreover, there are high values of overall accuracy (OA) for correlation between parts of the seams with high values of ash which are 47.86% and 39.81% for C_1 and B_2, respectively, and ash coals obtained by geological data.

© 2014 Elsevier B.V. All rights reserved.

1. Introduction

Recognition of coking coal parts in the bituminous coal seams is necessary for mine planning and equipment selection used for mining these seams. Ash and sulfur values are important for determination of proper coal quality for coke production regarding environmental control of coal mining (Younger, 2004). Conventional methods for modeling of various parts of coking coal are based on petrographical, physical, technological and geochemical studies especially measuring of sulfur and ash variations in the coal seams considering Russian standards and USGS system (Ahangaran et al., 2011; Brownfield et al., 2001; Wood and Kehn, 1976). The classifications based on all physical, mechanical, chemical, and technological characteristics of organic fraction of coal have been utilized in Iran since 1960s.

Geostatistical simulation has been widely used in geology and mining engineering to assess the uncertainty at un-sampled locations and to develop model the continuous variables (Emery and Lantuéjoul, 2006). Conditional simulation is designed initially to overcome the smoothing effect of kriging estimator especially when mapping sharp or extreme spatial discontinuities is looked for (Deutsch and Journel, 1998; Leuangthong et al., 2004; Soltani et al., 2014).

The simulation algorithms take into account both the spatial variation of actual data at sampled locations and the variation of estimates at un-sampled locations which means that simulation reproduces the sample statistics (histogram and semi-variogram model) and honors sample data at their original locations. Therefore, a simulation map represents the spatial distribution of the particular more realistic than a kriged map (Asghari and Madani Esfahani, 2013; Soltani et al., 2014). The geostatistical simulation is an alternative to the

* Corresponding author at: Department of Mining Engineering, South Tehran Branch, Islamic Azad University, Tehran, Iran.
E-mail addresses: P_afzal@azad.ac.ir, p.afzal@exeter.ac.uk (P. Afzal).

http://dx.doi.org/10.1016/j.coal.2014.03.003
0166-5162/© 2014 Elsevier B.V. All rights reserved.

conventional approaches of estimation which is independent of over and under estimation. This benefit is an important issue in order to apply for the fractal model and could reproduce better results.

Fractal/multifractal modeling, established by Mandelbrot (1983) has been widely used in geosciences specifically for interpretation of geochemical data spatial distribution and delineation of mineralized zones from barren host rocks since 1980s (Afzal et al., 2011, 2013; Agterberg

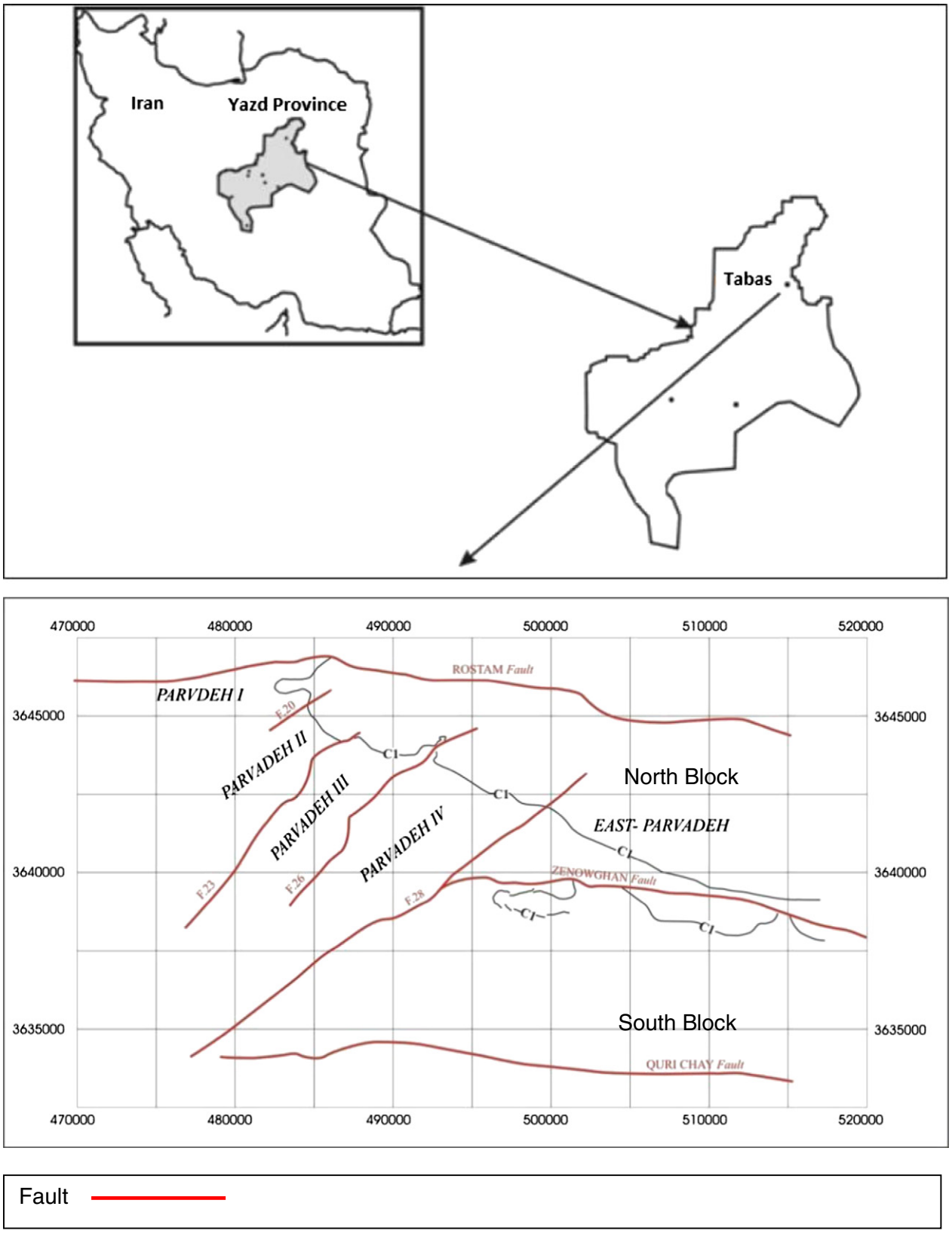

Fig 1. Location of Parvadeh deposits and East-Parvadeh blocks in the Iran and Tabas coalfield (Ahangaran et al., 2011).

et al., 1993, 1996; Cheng, 2007; Cheng et al., 1994; Costa, 1997; Costa and Dimitrakopoulos, 1998; Daneshvar Saein et al., 2012; Li et al., 2003; Turcotte, 1997; Yasrebi et al., 2013; Zuo et al., 2009; 2012, 2013). Cheng et al. (1994) and Cheng (1995) proposed concentration–area (C–A) and concentration–perimeter (C–P) fractal models for separation of geochemical anomalies from background and calculation of elemental

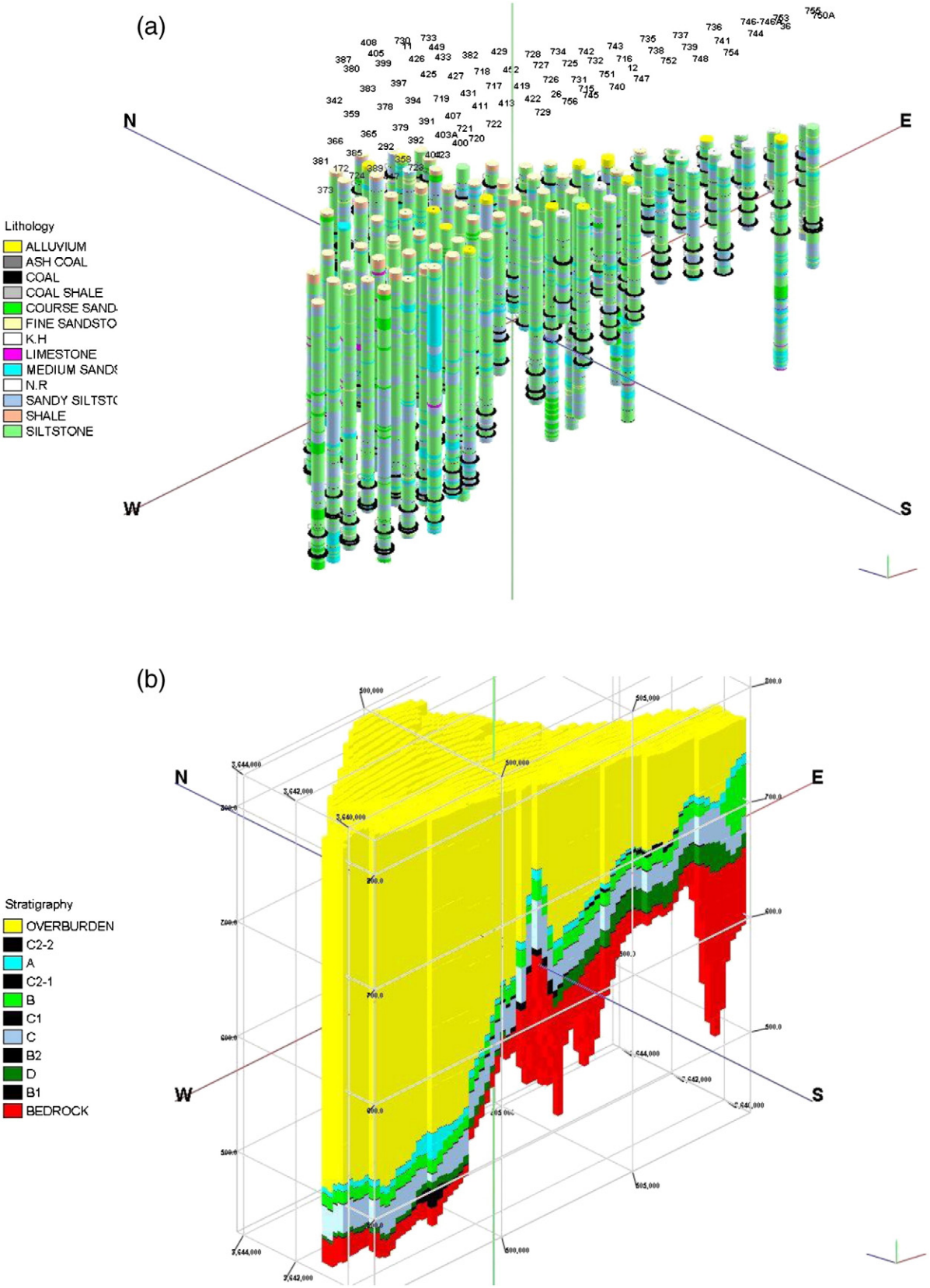

Fig. 2. Isometric view of drill hole locations (a) and a 3D geological model for the East-Parvadeh deposit with a vertical exaggeration equal to 30 (b).

threshold values for different geochemical data. Moreover, other fractal models were developed and applied in geochemical exploration such as number–size (N–S) by Mandelbrot (1983), power spectrum–area (S–A) by Cheng et al. (1999), concentration–distance (C–D) by Li et al. (2003), concentration–volume (C–V) by Afzal et al. (2011) and concentration–number (C–N) by Afzal and Hassanpour (2013).

In this paper, the turning bands simulation and C–V fractal model were applied to outline sulfur and ash populations for separation of high quality coking coals based on drillcore data from the C_1 and B_2 seams of the North block of East-Parvadeh coal deposit located in the Central Iran. Moreover, the results obtained by the fractal modeling were compared with USGS system (Wood and Kehn, 1976) and geological particulars by logratio matrix proposed by Carranza (2011).

2. C–V fractal model

The application of fractal models for analysis of mineralized zones was based on relationships between ore grades and volumes or tonnages (Afzal et al., 2013; Agterberg et al., 1993; Sadeghi et al., 2012; Sim et al., 1999; Yasrebi et al., 2013). Afzal et al. (2011) proposed the C–V fractal model for delineating different porphyry-Cu mineralized zones from barren host rocks. This model is as follows:

$$V(\rho \le \upsilon) \propto \rho^{-a1}; V(\rho \ge \upsilon) \propto \rho^{-a2} \quad (1)$$

where $V(\rho \le \upsilon)$ and $V(\rho \ge \upsilon)$ indicate two volumes with concentration values less than or equal to and greater than or equal to the contour value ρ; υ ,a1 and a2 represent the threshold value of a zone and fractal dimensions respectively. Threshold values in this model represent boundaries between different mineralized zones and barren host rocks of different ore deposits. To calculate $V(\rho \le \upsilon)$ and $V(\rho \ge \upsilon)$, that are the volumes enclosed by a contour level ρ in a 3D model, the borehole data of ore element concentrations were calculated using turning bands simulation (Emery and Lantuéjoul, 2006).

3. Turning bands simulation

The most applicable and widespread approximate algorithm is the sequential Gaussian (Deutsch and Journel, 1992) and continuous spectral methods (Shinozuka and Jan, 1972). These two approaches have some limitations and drawbacks (Chilès and Delfiner, 2012; Dehdari and Deutsch, 2012; Emery, 2004; Lantuéjoul, 2002). Another alternative is the turning bands method, which was first introduced by Chentsov (1957) in a special case of Brownian random functions but has been extended to the simulation of stationary and intrinsic random functions by Matheron (1973). This method aims at simplifying the simulation problem in multidimensional spaces, using simulations in one dimension and spreading them to the 2D or 3D space. This method is extremely fast with parallelizable computations and one can simulate as many locations as desired. The simulation also exactly reproduces the desired covariance. Actually, this method can be incorporated in both cases of stationary and intrinsic random function of order k (Emery and Lantuéjoul, 2006; Chilès and Delfiner, 2012). The proposed simulation algorithm in this study is based on a former code published by Lantuéjoul (1994), which has been completed by Emery and Lantuéjoul (2006) to include the following features:

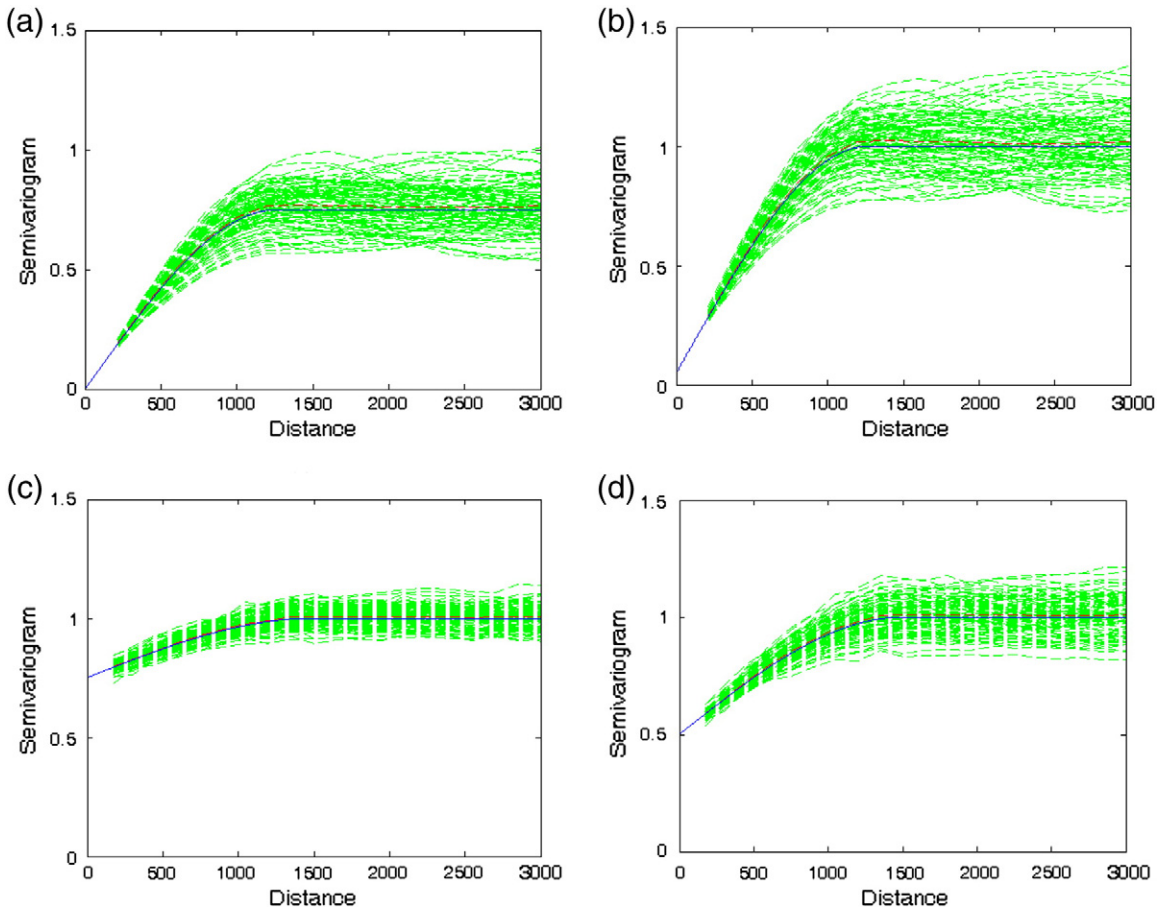

Fig. 3. Reproduced variograms for 100 realizations of: a) ash in B_2; b) sulfur in B_2; c) ash in C_1 and d) sulfur in B_2 (green line: experimental variogram for each realization; red line: mean of experimental variogram over 100 realizations; blue line: theoretical variogram of normal score transformed variables).

- To handle isotropic covariance models,
- To simulate gridded locations on large domains,
- Accurate reproduction of the desired covariance model (without approximation),
- Availability of the most commonly used covariance models,
- Conditioning to a set of existing data,
- Definition of either a unique or a moving,
- Neighborhood for conditioning kriging,
- Back-transformation from normal values to original units.

4. Geological setting

Iranian coking coal resources and reserves are estimated to be about 7–10 Gt that is mainly located in two major basins in Northern and Central Iran, namely Alborz and the Central basins respectively (Solaymani and Taghipour, 2012). The Tabas coalfield provides most of Iran's coking coal for metallurgical applications, as its reserve is estimated to be 3–4 Gt (Afzal et al., 2008; Ahangaran et al., 2011; Moore and Esmaeili, 2012; Yazdi and Esmaeilnia, 2004).

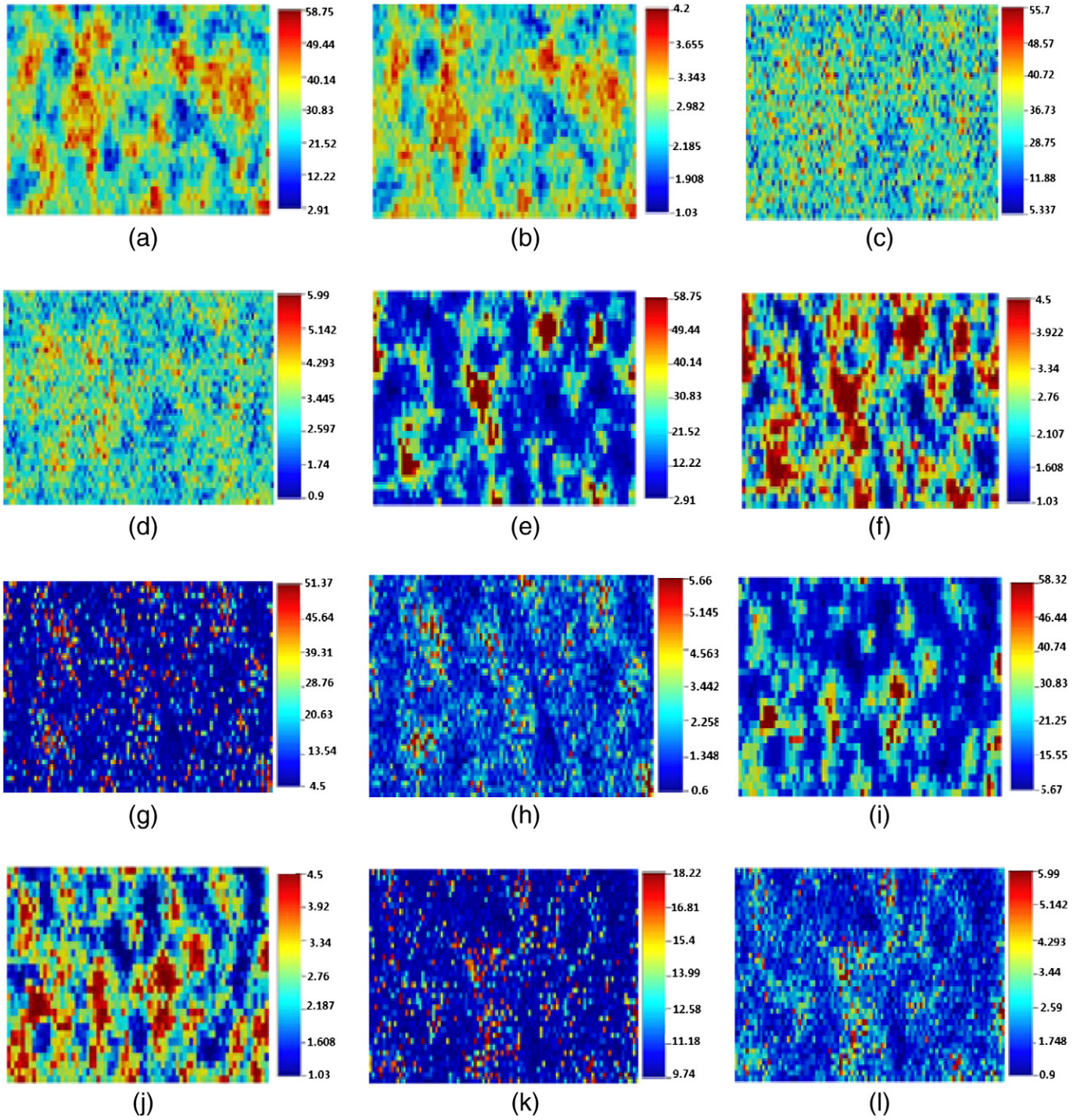

Fig. 4. E-types for a) ash in B_2; b) sulfur in B_2; c) ash in C_1 and d) sulfur in C_1; realization # 20 for e) ash in B_2; f) sulfur in B_2; g) ash in C_1 and h) sulfur in C_1; and realization # 100 for i) ash in B_2; j) sulfur in B_2; k) ash in C_1 and l) sulfur in C_1.

The East-Parvadeh coal deposit is located about 80 km south of the Tabas region, Central Iran (Fig. 1). The Tabas coalfield district is a part of Central Iran's structural zone that is divided into different sub-zones namely Parvadeh, Nayband and Mazinu. The Parvadeh area includes six parts divided by major faults and the East-Parvadeh is depicted in Fig. 1. The East-Parvadeh coal deposit is divided by Zenoughan fault to the North and South blocks. According to dip, depth and structural effects, the North block has better quality coal seams than the South block. The coal bearing strata of the Tabas coalfield consist mainly of sediments of Upper Triassic, Middle Jurassic age especially for the Nayband formation and Ghadir member. Their rock units include siltstone, sandstone, shale, sandy siltstone and small amounts of limestone and ash coal which is coal with high values of ash. Coal seams in the Parvadeh region are named A, B, C, D, E and F; worth noting that B and C coal seams are minable based on their quality and quantity, specially C_1 and B_2 seams which have better quality (Fig. 2).

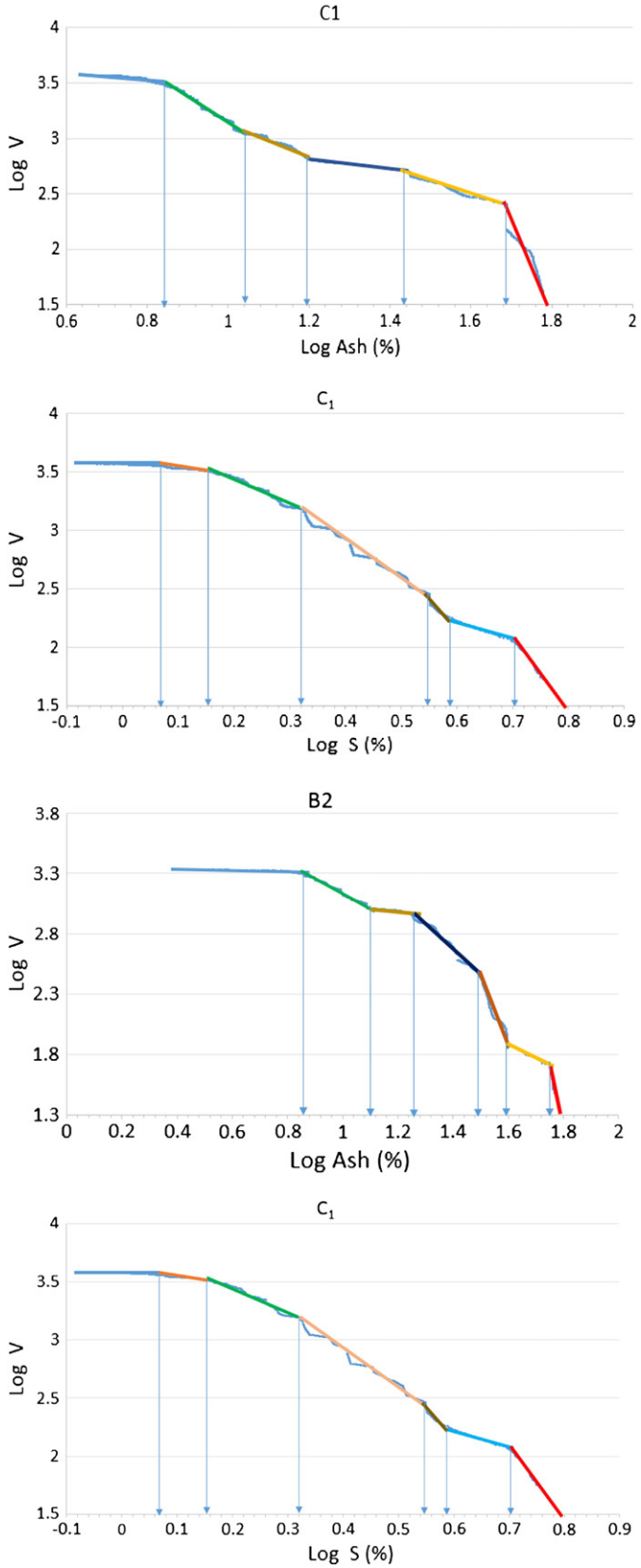

Fig 5. C–V log–log plots of sulfur and ash for C_1 and B_2 seams in the North block of East-Parvadeh deposit based on realization # 20 (different lines show various geochemical population).

Table 1
Different geochemical populations for sulfur in C_1 seam based on C–V fractal modeling.

Category	Very low	Low	Moderate	Relatively high	High	Very high
Sulfur	<1.41	1.41–2.09	2.09–3.55	3.55–3.89	3.89–5.01	>5.01

A geological 3D model of the coal seams was generated by utilizing RockWorks™ v. 15 software and surface/subsurface data collected from surface outcrops and drillcores. The data used include collar coordinates of drill holes, azimuth and dip (orientation), stratigraphy and sulfur and ash values for the coal seam cores. Additionally, other surface data consist of topographical data, faults, outcrops of coal seams and other geological features which are relevant to constructing of the 3D geological model. Coal seams were delineated in all drillcores with respect to geological logging consisting of petrographic and mineralogical studies. The Triangulation algorithm was used for seam modeling and after 3D modeling of coal seams showing coal seams are deeper in the SW part of the area (Fig. 2).

5. Simulation of ash and sulfur values based on turning bands

For this study, 87 and 54 samples were collected from 87 drillcores from the C_1 and B_2 coking coal seams respectively and also chemical analysis for evaluation of sulfur and ash content in these samples was carried out. The area study comprises 14,500 m, 5500 m and 520 m along X, Y and Z respectively considering the deposit geometric properties. Subsequently, block size was determined based on grid drilling dimensions of 250 m × 250 m × 0.2 m for X, Y and Z respectively (David, 1970). The 3D models consisting of sulfur and ash distribution in the C_1 and B_2 seams were created using turning bands conditional simulation.

The ash and sulfur data have been transformed by using a normal score transformation and the statistics of transformed data check the correctness of the transformation, and also, the experimental semi-variogram and a spherical model fitted to the raw and normal transformed data. Turning bands simulation and visualizations were carried out with a MATLAB code which proposed by Emery and Lantuéjoul (2006) and SGeMS software. The histogram and semi-variogram model reproduced over a number of realizations should be, on average, equal to the sample statistics (Emery and Gonzalez, 2007) that reproduced variograms were represented in Fig. 3. Based on the simulation, 100 realizations of ash and sulfur spatial distributions are generated in the C_1 and B_2 seams. Horizontal plan of two randomly selected realizations consisting of realizations of 20 and 100 within E-type (average of all realizations) is displayed in Fig. 4. For the simulation

Table 2
Different geochemical populations for ash in C_1 seam based on C–V fractal modeling.

Category	Very low	Low	Moderate	Relatively high	High	Very high
Ash	<6.92	6.92–10.96	10.96–15.85	15.85–27.54	27.54–47.86	>47.86

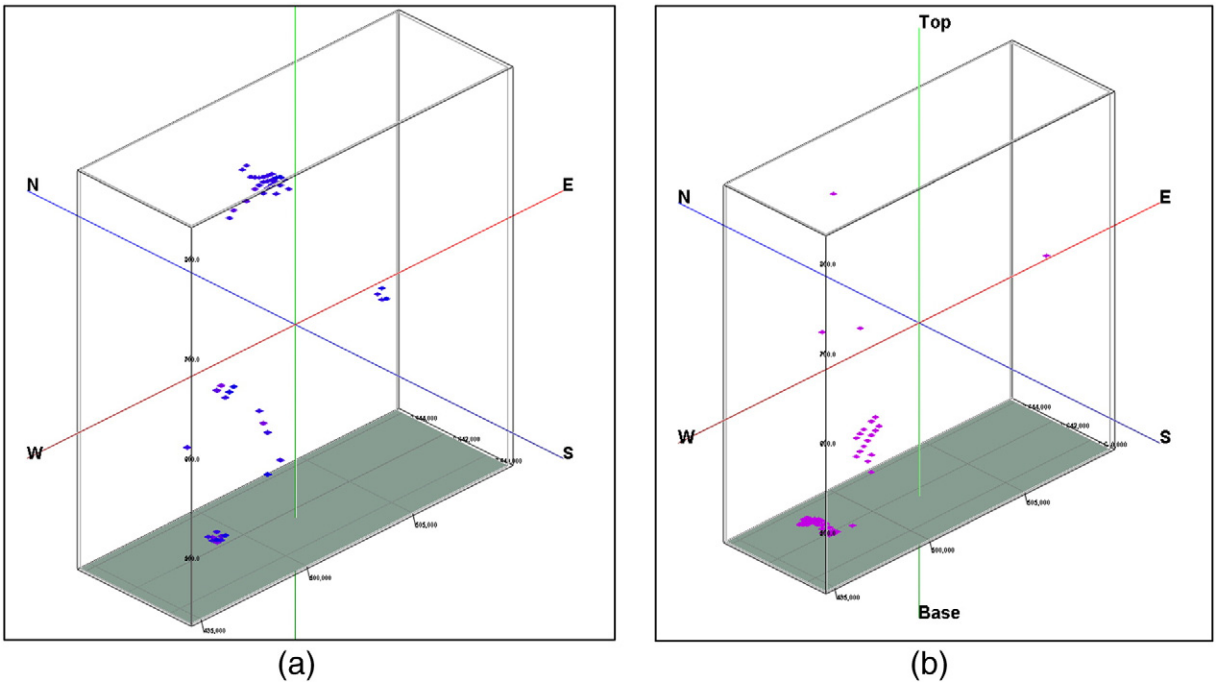

Fig 6. Proper populations for sulfur (<1.41%: a) and ash (<6.92%: b) in C_1 seam based on C–V fractal modeling in North block of the East-Parvadeh coal deposit.

process, in order to fasten the convergence to the multiGaussian distribution, the equi-distributed directions are considered as 1000 bands. As can be seen from Fig. 3, the experimental variogram of realizations and its mean could reproduce exactly the theoretical variogram of the normal score transformed variables. The histograms also reproduced the experimental histogram of normal score transformed variables, but they are not presented here to save the spaces. In Fig. 4, some realizations of C_1 seams are not structured properly because of the theoretical variogram fitted to the experimental variogram of the normal score transformed variables. This issue can be due to the low number of samples, not having a good structure for the ash content and sulfur from the geological standpoint. This ambiguity can be resolved in the further steps of core drilling and obtaining new representative samples from the C_1 seam.

6. Application of C–V fractal modeling

The C–V log–log plots were built up for sulfur and ash data in the C_1 and B_2 seams based on realization # 20 because all realizations have a similar range with an equal amount for maximum and minimum data and one of them could be used randomly (Fig. 5). Their breakpoints between straight-line segments in the log–log plots represent threshold values for separating of various sulfur and ash populations in the both seams. The straight fitted lines were resulted based on least-square regression in the log–log plots (Agterberg et al., 1996; Spalla et al., 2010). Based on the C–V log–log plots for C_1 seam, there are seven and six different geochemical populations for sulfur and ash respectively (Tables 1 and 2). C_1 seam with sulfur values lower than 1.41% can be categorized as good and relatively good populations for coking coal via USGS system (Wood and Kehn, 1976). These populations are located in the northern and western parts of the seam (Fig. 6). Populations with lowest quality for coking coal which have sulfur values higher than 3.89% were determined as undesirable populations and also sulfur values higher than 3.89% can show pyritic veins in the coal seam. Proper populations for ash in the C_1 seam have ash value lower than 6.92% that presents good populations for coking coal due to USGS system. These populations are located mostly in the western parts of the seam (Fig. 6). Populations with lowest quality for coking coal have ash values higher than 15.85% and last population with ash higher than 47.86% can indicate ash coals. Based on the C–V log–log plots for B_2 seam, there are seven different geochemical populations for sulfur and ash data (Tables 3 and 4). Suitable populations for sulfur in B_2 seam have sulfur values lower than 1.55% which reveal high quality population for coking coal according to USGS system (Table 5). This population (with sulfur lower than 1.55%) is situated mostly in the western, central and northern parts of the seam (Fig. 7). Populations with low quality for coking coal have sulfur values higher than 3.98% which can be correlated with pyritic veins. Proper populations for ash in B_2 seam are less than 6.39% which is in the western, northern and central parts of the seam (Fig. 7). Populations with low quality for coking coal contain ash higher than 39.81%.

7. Local uncertainty for results of C–V modeling

It is intuitive that the values of the data close to a location modify the prior probability distribution: the probability to exceed a cut-off is greater in high-value areas than in low-value areas. However, the uncertainty associated with the unknown value at that location decreases

Table 3
Different geochemical populations for sulfur in B_2 seam based on C–V fractal modeling.

Category	Very low	Low	Moderate	Relatively high	High	Very high
Sulfur	<1.55	1.55–2.24	2.24–2.95	2.95–3.38	3.38–3.98	>3.98

Table 4
Different geochemical populations for ash in B_2 seam based on C–V fractal modeling.

Category	Very low	Low	Moderate	Relatively high	High	Very high
Ash (%)	<6.39	6.39–12.58	12.58–18.20	18.20–30.20	30.20–39.81	>39.81

Table 5
Coking coal categorization based on the USGS system (Wood and Kehn, 1976).

Category	Low ash	Medium ash	High ash
Ash (%)	<8%	8%–15%	>15%
Category	Low sulfur	Medium sulfur	High sulfur
Sulfur (%)	<1.5%	1.5%–3%	>3%

when data exist near that location. To take into account the information brought by the data, one uses the concept of "conditional" (or "posterior") cumulative distribution function (ccdf). Now, the probability to exceed a threshold z depends on that location under consideration (hence the name of local uncertainty model), through the values of the data close to this location and the positions of these data.

The local uncertainty models allow taking decision in the presence of uncertainty and calculating the risks of taking an incorrect decision (Chilès and Delfiner, 2012). The simulations provide a set of plausible scenarios and allow assessing the local uncertainty in the spatial distribution of the continuous variables within the deposit. In particular, one can characterize these domains by mapping their probabilities of occurrence at each location of the deposit (in practice, their frequencies of occurrence over the simulations: Emery and Gonzalez, 2007). The probability maps were obtained to account for the drill hole information and for the thresholds obtained from the C–V fractal modeling can be depicted in Fig. 8. As can be seen, these probability maps are quantified for the limitation less than the first threshold obtained by the C–V fractal modeling. The calculated values for local uncertainty are lower than 0.34 associated with low values of ash and sulfur in the coal seams, as depicted in Fig. 8. For example, in the West-North part of the B_2 seam map, the probability of ash content less than 6.92% is high (approximately between 60% and 100%). Therefore, the productive areas have been assessed by these local uncertainty maps associated with the fractal model in the underlying coal seam.

8. Correlation between C–V fractal modeling and geological particulars

The multifractal nature of C–V log–log plots can be illustrated in different stages for coalification. First stage could exist in coals with ash values higher than 47.86% and 39.81% for C_1 and B_2, respectively. The stage could be revealed with ash coals and pyritic veins in the area (Fig. 9). In this stage, values of sulfur are high in the coals which are higher than 3% based on C–V fractal modeling for both coal seams. Main stage of coalification based on the C–V modeling for both ash and sulfur content is lower than 7% and 1.6%.

Carranza (2011) proposed an analysis for calculation of overlaps or spatial correlations between two binary models e.g., geological and mathematical models such as fractal or geostatistical modeling. As a result, a model with four overlap conditions was achieved to obtain numbers of voxels (performance of binary geochemical distribution modeling) corresponding to each of the four classes of overlap zones. Voxels' numbers of overlap conditions between two binary models are utilized to determine overall accuracy (OA), and types I & II errors (TEI and TEII). OA, TEI and TEII relate to the ability of the analysis to mineralized zones (Table 6).

Correlation between the C–V fractal modeling and pyritic veins and ash coals for the coking coal seams (Fig. 9) was achieved by logratio matrix. Undesirable populations for sulfur and ash (variables) in the C_1 and B_2 seams based on the turning bands simulation and C–V fractal modeling correlated with pyritic veins and ash coals which derived via by geological modeling respectively. Four overlap parameters namely A, B, C and D for two variables in two seams were defined. Finally, the logratio matrix was generated by placing the four parameters and also calculation of TEI, TEII and OA was performed (Tables 7–10). Comparison between OAs for high values of sulfur in C_1 and B_2 seams and pyritic veins shows that there is a good correlation between both of them which is 0.84 (Tables 7 and 9). Moreover, there are high values of OAs between ash coals and high ash populations derived via C–V fractal modeling which illustrate a proper correlation between C–V fractal and geological modeling. These high ash populations which are

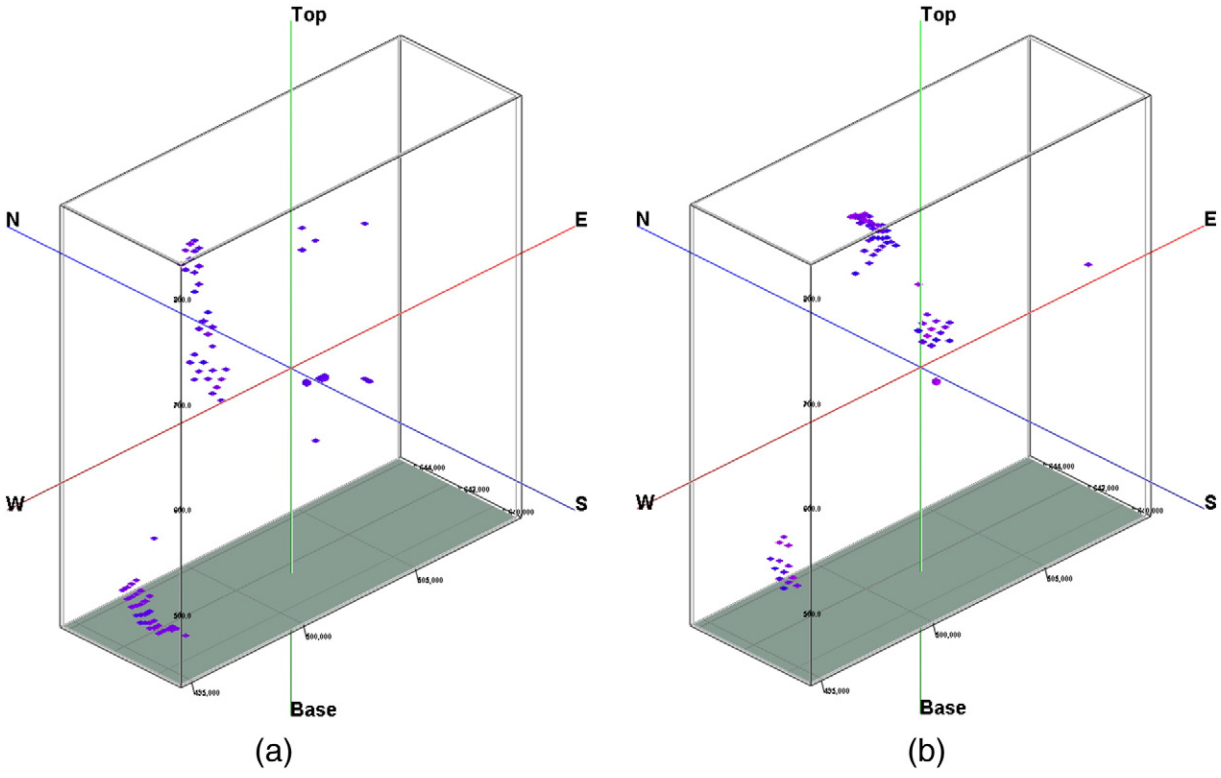

Fig 7. Proper populations for ash (<6.39%: a) and sulfur (<1.55%: b) populations for ash in B_2 seam based on C–V fractal modeling in the North block of the East-Parvadeh coal deposit.

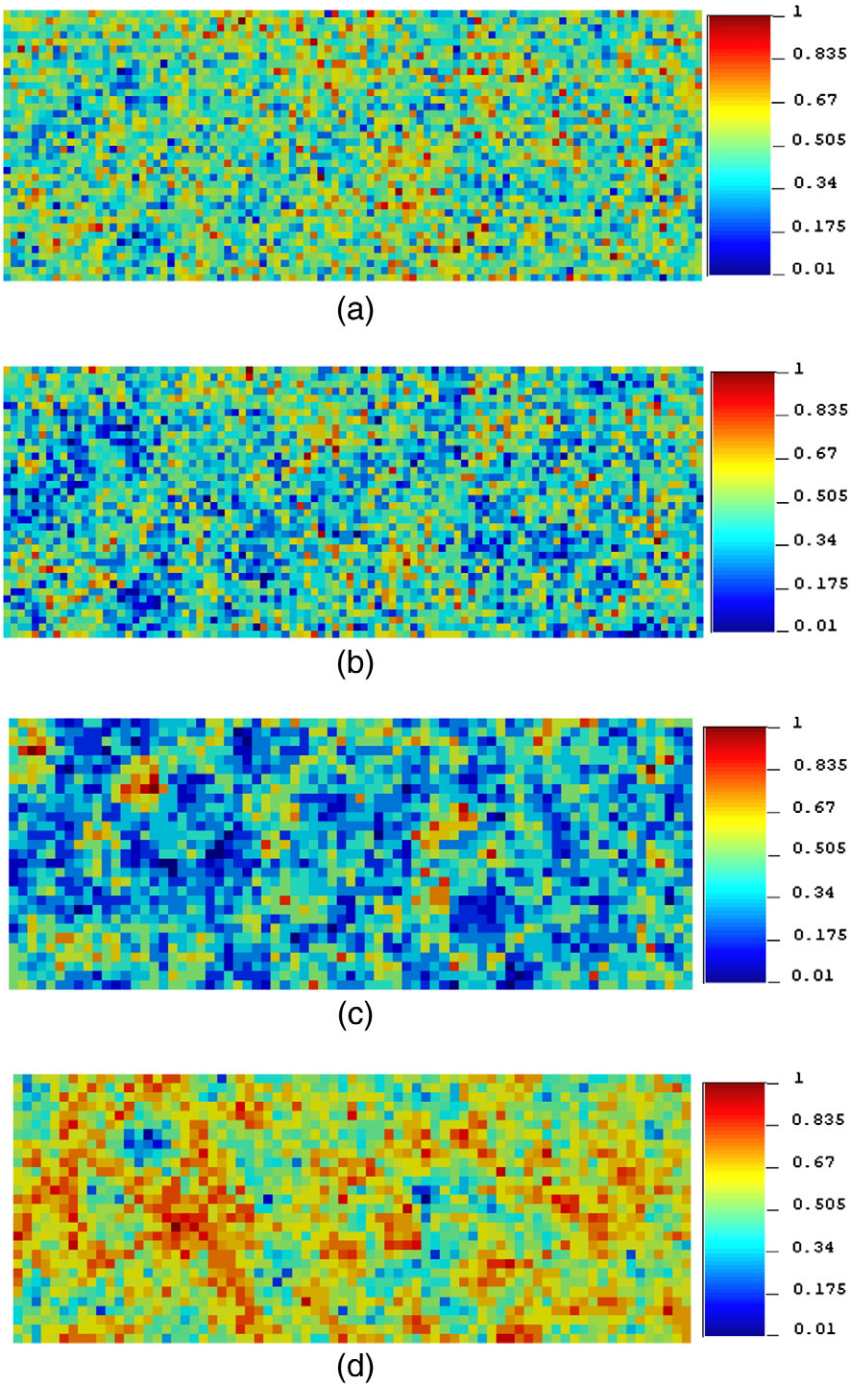

Fig 8. Local uncertainty (probability map) for high quality parts in C_1 (ash < 6.39%: a; sulfur < 1.55%: b) and B_2 (ash < 6.92%: c; sulfur < 1.41%:d) seam based on C–V fractal modeling in North block of the East-Parvadeh coal deposit.

47.86% and 39.81% for C_1 and B_2, respectively, can be shown in the first stage of coalification with low quality.

9. Conclusion

In this study, the turning bands simulation and C–V fractal modeling were utilized to outline different qualities for the C_1 and B_2 coal seams in terms of sulfur and ash values in the North block of East-Parvadeh coking coal deposit, Central Iran. Investigation of the deposit reveals that results obtained by the geostatistical simulation can be used for the outlining of high quality coking coal by fractal modeling. The highest quality for coking coal in C_1 seam considering the less sulfur and ash corresponds to the populations lower than 1.41% and 6.92% respectively. The desirable populations considering obtained breakpoints based on C–V log–log plot for B_2 seam with proper quality are lower than 1.55% and 6.39% sulfur and ash respectively. Desirable populations for both seams are located mostly in the central, northern and western parts of the studied area. The uncertainty maps for the populations indicate that there are low values of uncertainty that resulted high quality of coking coals. Furthermore, the obtained results support the coal categorization by USGS system. Correlation between results and pyritic veins and ash coals obtained by geological modeling

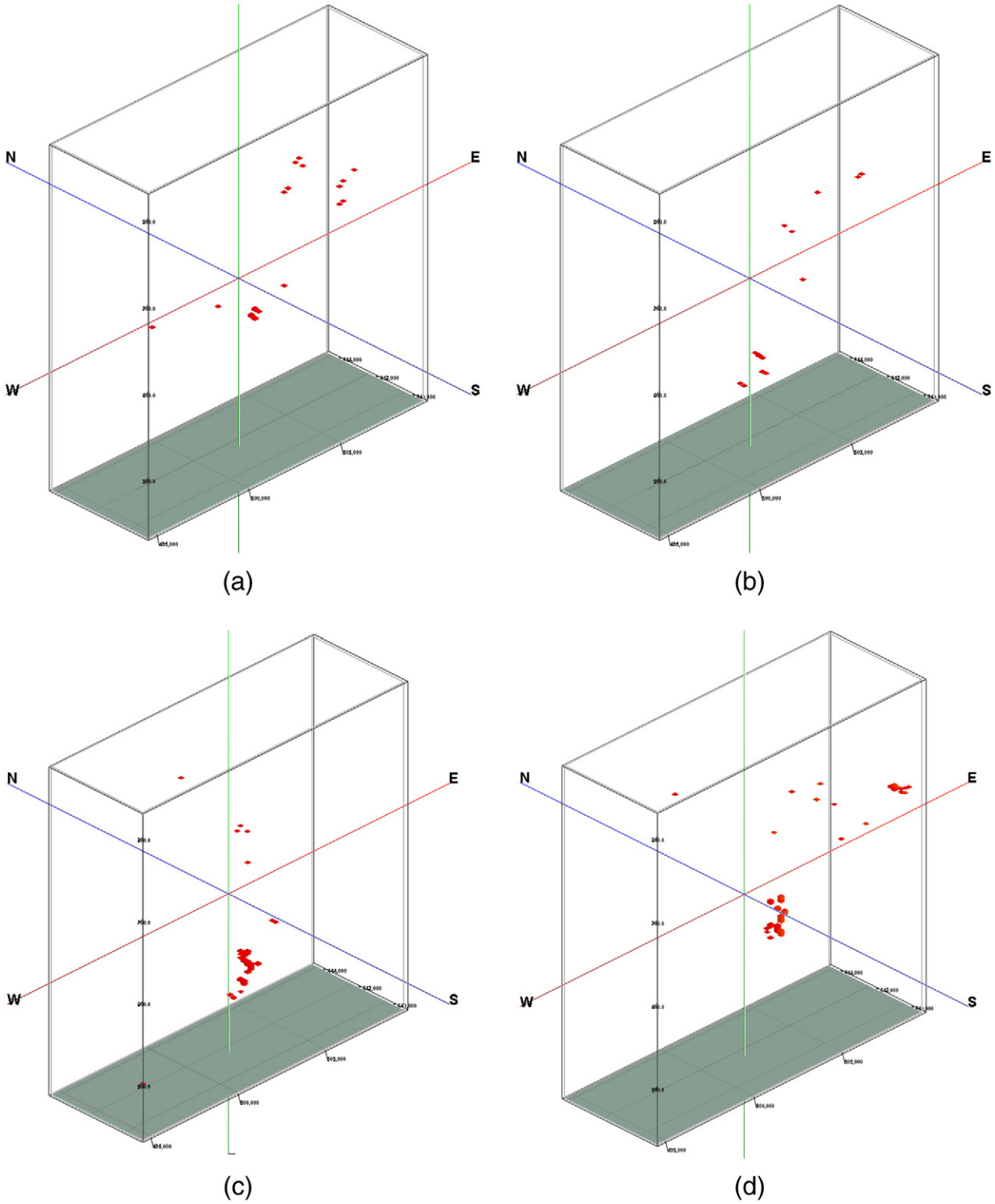

Fig 9. Pyritic veins in C_1 (a) and B_2 (b) and ash coals in the C_1 (c) and B_2 (d).

Table 6
Matrix for comparing performance of fractal modeling results with Russian model.

		Geological model	
		Inside zone	Outside zone
Fractal model	Inside zone	True positive (A)	False positive (B)
	Outside zone	False negative (C)	True negative (D)
		Type I error = C / (A + C)	Type II error = B / (B + D)
		Overall accuracy = (A + D) / (A + B + C + D)	

A, B, C and D represent numbers of voxels in overlaps between classes in the binary model results of fractal and geological models (Carranza, 2011).

Table 7
Logratio matrix for high value sulfur population and pyritic veins in C_1 seam from North block of East-Parvadeh coal deposit.

		Pyritic veins from geological model	
		Inside pyritic veins	Outside pyritic veins
Fractal model	Inside zone (S > 3.89%)	71	320
	Outside zone (S > 3.89%)	3	1554
		TEI error = 0.04	TEII error = 0.36
		OA = 0.834	

Table 8
Logratio matrix for high value ash population and ash coals in C_1 seam from the North block of East-Parvadeh coal deposit.

		Ash coals from geological model	
		Inside ash coals	Outside ash coals
Fractal model	Inside zone (ash > 47.86%)	29	2
	Outside zone (ash < 47.86%)	3	1914
		TEI error = 0.093	TEII error = 0.001
		OA = 0.997	

Table 9
Logratio matrix for high sulfur population and pyritic veins in B_2 seam from North block of East-Parvadeh coal deposit.

		Pyritic veins in geological model	
		Inside pyritic veins	Outside pyritic veins
Fractal model	Inside zone (S > 3.38%)	76	553
	Outside zone (S < 3.38%)	9	2907
		TEI error = 0.105	TEII error = 0.159
		OA = 0.841	

Table 10
Logratio matrix for high ash population and ash coal in B_2 seam from North block of East-Parvadeh coal deposit.

		Ash coals from geological model	
		Inside ash coals	Outside ash coals
Fractal model	Inside zone (ash > 39.81%)	491	52
	Outside zone (ash < 39.81%)	6	2944
		TEI error = 0.23	TEII error = 0
		OA = 0.983	

shows that there are good correlation between low quality coal parts derived via fractal modeling. Moreover, OAs between fractal and geological modeling are high values especially for ash coals. As a result, the combination of fractal model and geostatistical simulation as an alternative to the conventional method of estimation such as kriging or Inverse Distance could reproduce more reliable results and one can have a better interpretation on the productive areas in coal seams to make a proper decision.

Acknowledgments

The authors would like to thank Mr. Masoud Hoseini and Ms Zahra Ebrahimi from Iran Minerals Production & Supply Co. (IMPASCO) for authorizing the access to the East-Parvadeh drillcores and dataset.

References

Afzal, P., Hassanpour, Sh., 2013. Application of concentration–number (C–N) multifractal modeling for geochemical anomaly separation in Haftcheshmeh porphyry system, NW Iran. Arab. J. Geophys. Res. 6, 957–970.
Afzal, P., Alvan Darestani, R., Ahangaran, D.K., 2008. 3D modelling and reserve evaluation of mineable coal seams in East-Parvadeh coal deposit, Tabas, Central Iran. Proceeding of 21st World Mining Congress and Expo 2008, Poland, pp. 7–12.
Afzal, P., FadakarAlghalandis, Y., Khakzad, A., Moarefvand, P., Rashidnejad Omran, N., 2011. Delineation of mineralization zones in porphyry Cu deposits by fractal concentration–volume modeling. J. Geochem. Explor. 108, 220–232.
Afzal, P., Dadashzadeh Ahari, H., RashidnejadOmran, N., Aliyari, F., 2013. Delineation of gold mineralized zones using concentration–volume fractal model in Qolqoleh gold deposit, NW Iran. Ore Geol. Rev. 55, 125–133.
Agterberg, F.P., Cheng, Q., Wright, D.F., 1993. Fractal modeling of mineral deposits. In: Elbrond, J., Tang, X. (Eds.), 24th APCOM Symposium Proceeding. Montreal, Canada, pp. 43–53.
Agterberg, F.P., Cheng, Q., Brown, A., Good, D., 1996. Multifractal modeling of fractures in the Lac du Bonnet Batholith, Manitoba. Comput. Geosci. 22, 497–507.
Ahangaran, D.K., Afzal, P., Yasrebi, A.B., Wetherelt, A., Foster, P.J., Alvan Darestani, R., 2011. An evaluation of the quality of metallurgical coking coal seams within the north block of East-Parvadeh coal deposit, Tabas, Central Iran. J. Miner. Metall. 47 (A), 1–16.
Asghari, O., Madani Esfahani, N., 2013. A new approach for the geological risk evaluation of coal resources through a geostatistical simulation. Arab. J. Geosci. 6, 929–943.
Brownfield, M.E., Steinshouer, D.W., Povarennykh, M.Y., Eriomin, I., Shpirt, M., Meitov, Y., Sharova, I., Goriunova, N., Zyrianova, M.V., 2001. Coal quality and resources of the former Soviet Union — an ArcView Project. U.S.G.S. Open-File Report 01-104.
Carranza, E.J.M., 2011. Analysis and mapping of geochemical anomalies using log ratio-transformed stream sediment data with censored values. J. Geochem. Explor. 110, 167–185.
Cheng, Q.M., 1995. The perimeter–area fractal model and its application to geology. Math. Geol. 27, 69–82.
Cheng, Q., 2007. Mapping singularities with stream sediment geochemical data for prediction of undiscovered mineral deposits in Gejiu, Yunnan Province, China. Ore Geol. Rev. 32, 314–324.
Cheng, Q., Agterberg, F.P., Ballantyne, S.B., 1994. The separation of geochemical anomalies from background by fractal methods. J. Geochem. Explor. 51, 109–130.
Cheng, Q., Xu, Y., Grunsky, E., 1999. Integrated spatial and spectral analysis for geochemical anomaly separation. In: Lippard, S.J., Naess, A., Sinding-Larsen, R. (Eds.), Proc of the Conference of the International Association for Mathematical Geology. , vol. 1, pp. 87–92 (Trondheim, Norway).
Chentsov, N.N., 1957. Levy Brownian motion for several parameters and generalized white noise. Theory Probab. Appl. 2 (2), 265–266.
Chilès, J.P., Delfiner, P., 2012. Geostatistics: Modeling Spatial Uncertainty. Wiley, New York.
Costa, J.F., 1997. Development in Recoverable Reserves and Ore Body Modeling. (PhD thesis in) WH Bryan Mining Geology Research Centre: University of Queensland, Brisbane, Australia.
Costa, J.F., Dimitrakopoulos, R., 1998. A conditional fractal (fBm) simulation approach for orebody modelling. Int. J. Surf. Min. Reclam. Environ. 12, 197–202.
Daneshvar Saein, L., Rasa, I., Rashidnejad Omran, N., Moarefvand, P., Afzal, P., Sadeghi, B., 2012. Application of number–size (N–S) fractal model to quantify of the vertical distributions of Cu and Mo in Nowchun porphyry deposit (Kerman, SE Iran). Arch. Min. Sci. J. 58, 89–105.
David, M., 1970. Geostatistical Ore Reserve Estimation. Elsevier, Amsterdam (283 pp.).
Dehdari, V., Deutsch, C.V., 2012. Applications of randomized methods for decomposing and simulating from large covariance matrices. Geostatistics Oslo 2012. Quantitative Geology and Geostatistics, 17, pp. 15–26.
Deutsch, C.V., Journel, A.G., 1992. GSLIB: Geostatistical Software Library and User's Guide. Oxford University Press, New York p. 340.
Deutsch, C., Journel, A.G., 1998. GSLIB: Geostatistical Software Library and User's Guide Second Edition. Oxford University Press, New York (340 pp.).
Emery, X., 2004. Testing the correctness of the sequential algorithm for simulating Gaussian random fields. Stoch. Env. Res. Risk A. 18 (6), 401–413.
Emery, X., Gonzalez, K.E., 2007. Probabilistic modeling of mineralogical domains and its application to resources evaluation. J. South. Afr. Inst. Min. Metall. 107 (12), 803–809.
Emery, X., Lantuéjoul, Ch., 2006. TBSIM: a computer program for conditional simulation of three-dimensional Gaussian random fields via the turning bands method. Comput. Geosci. 32, 1615–1628.
Lantuéjoul, C., 1994. Non conditional simulation of stationary isotropic multiGaussian random functions. In: Armstrong, M., Dowd, P.A. (Eds.), Geostatistical Simulations. Kluwer Academic, Dordrecht, pp. 147–177.
Lantuéjoul, C., 2002. Geostatistical Simulation. Models and Algorithms, Springer, Berlin.
Leuangthong, O., McLennan, J.A., Deutsch, C.V., 2004. Minimum acceptance criteria for geostatistical realizations. Nat. Resour. Res. 13, 131–141.
Li, C., Ma, T., Shi, J., 2003. Application of a fractal method relating concentrations and distances for separation of geochemical anomalies from background. J. Geochem. Explor. 77, 167–175.
Mandelbrot, B.B., 1983. The Fractal Geometry of Nature. Freeman, San Fransisco (468 pp.).
Matheron, G., 1973. The intrinsic random functions and their applications. Adv. Appl. Probab. 5 (3), 439–468.
Moore, F., Esmaeili, A., 2012. Mineralogy and geochemistry of the coals from the Karmozd and Kiasar coal mines, Mazandaran province, Iran. Int. J. Coal Geol. 96–97, 9–21.
Sadeghi, B., Moarefvand, P., Afzal, P., Yasrebi, A.B., Daneshvar Saein, L., 2012. Application of fractal models to outline mineralized zones in the Zaghia iron ore deposit, Central Iran. J. Geochem. Explor. 122, 9–19.
Shinozuka, M., Jan, C.M., 1972. Digital simulation of random processes and its applications. J. Sound Vib. 25 (1), 111–128.
Sim, B.L., Agterberg, F.P., Beaudry, C., 1999. Determining the cutoff between background and relative base metal contamination levels using multifractal methods. Comput. Geosci. 25, 1023–1041.

Solaymani, Z., Taghipour, N., 2012. Petrographic characteristics and palaeoenvironmental setting of Upper Triassic Olang coal deposits in northeastern Iran. Int. J. Coal Geol. 92, 82–89.
Soltani, F., Afzal, P., Asghari, O., 2014. Delineation of alteration zones based on sequential Gaussian simulation and concentration–volume fractal modeling in the hypogene zone of Sungun copper deposit, NW Iran. J. Geochem. Explor. http://dx.doi.org/10.1016/j.gexplo.2014.02.007.
Spalla, M.I., Morotta, A.M., Gosso, G., 2010. Advances in Interpretation of Geological Processes: Refinement of Multi-Scale Data and Integration in Numerical Modelling. Geological Society, London (240 pp.).
Turcotte, D.L., 1997. Fractals and Chaos in Geology and Geophysics. Cambridge Univ, Press, Cambridge.
Wood, G.H., Kehn, M., 1976. Coal Resource Classification System of U.S. Geological Survey. Bulletin 1450-B. USGS. pp. 4–5.
Yasrebi, A.B., Afzal, P., Wetherelt, A., Foster, P.J., Esfahanipour, R., 2013. Correlation between geology and concentration–volume fractal models: significance for Cu and Mo mineralised zones separation in Kahang porphyry deposit, Central Iran. Geol. Carpath. 64, 153–163.
Yazdi, M., Esmaeilnia, S.A., 2004. Geochemical properties of coals in the Lushan coalfield of Iran. Int. J. Coal Geol. 60, 73–79.
Younger, P.L., 2004. Environmental impacts of coal mining and associated wastes: a geochemical perspective, geological society of London. Spec. Publ. J. 236, 169–209.
Zuo, R., Cheng, Q., Xia, Q., 2009. Application of fractal models to characterization of vertical distribution of geochemical element concentration. J. Geochem. Explor. 102, 37–43.
Zuo, R., Carranza, E.J.M., Cheng, Q., 2012. Fractal/multifractal modelling of geochemical exploration data. J. Geochem. Explor. 122, 1–3.
Zuo, R., Xia, Q., Wang, H., 2013. Compositional data analysis in the study of integrated geochemical anomalies associated with mineralization. Appl. Geochem. 28, 202–221.